Ceramics-Silikáty 67 (3), 348-359 (2023)
www.ceramics-silikaty.cz
doi: 10.13168/cs.2023.0035

FORMATION OF SILVER COLLOIDS ON THE TIN SIDE OF THE FLOAT GLASS

#ALEŠ MAREŠKA, TEREZA KORDOVÁ, MARTIN HAVLÍK MÍKA

Faculty of Chemistry and Technology, University of Chemistry and Technology, Prague,
Technická 5, Dejvice, 166 28 Praha 6. Czech Republic

#E-mail: mareskaa@vscht.cz

Submitted July 22, 2023; accepted August 18, 2023

Keywords: Glass, Automotive, Coating, Diffusion, Manufacturing, Lamination, Defects

During the float glass process in a float bath, tin diffuses into the surface of the glass. The final product of the float process has two sides – one tin side and the other air side of the glass. In the next step, a layer of material is applied to the air side of the glass, which most often has an anti-reflective function, consisting of several layers, where the primary function is performed by a layer of silver. Such glass is used in the construction or automotive industry, for example. A problem arises, however, if the float glass is processed by another process where the glass is heated. When the glass is reheated, defects may appear on the tin side of the float blank due to the diffusion of ions present on the tin side of the float glass to its surface. The article deals with the diffusion of silver on the tin side of float glass in the laboratory and the subsequent analysis of the defect. The goal is to discuss the mechanism of this phenomenon and the possible methods to prevent the defect from occurring.

INTRODUCTION

The formation of colloidal silver arises from the reprocessing of float glass when the coated glass is heated above the glass transition temperature, a standard temperature of around 560 °C which is subsequently cooled to room temperature [1]. The glass must contain tin, selenium or tellurium, or lead, which, in this case, serves as a reducing agent. Due to the presence of the reducing agent, silver ions Ag^+ ill be reduced to the metal state Ag^0 [2].

Doremus [3] described the diffusion of silver ions Ag^+ into nucleation sites where colloidal Ag^0 particles grow. This reaction is due to the chemical reactions between diffuse oxygen and Sn^{2+} in the region close to the glass surface. The silver diffusion is affected by the presence of Sn^{2+} ions. In the glass surface, chemical reactions take place between the Ag^+ and Sn^{2+} ions, which lead to the precipitation of Ag^0 nanometre crystals. The typical yellow colour of the crystals is due to the surface plasmon resonance of the Ag^0 crystals. The plasmon resonance of the crystals is significantly different between the air side of the glass and the tin side of the glass due to the differences in the nucleation and growth processes associated with Ag crystals [4].

The formation of colloidal silver on the tin side of float glass is related to the concentration and chemical status of tin on the glass surface [5]. The concentration of the tin first decreases in the first 10 mm of the glass and then manifests itself with a long end, reaching up to 30 mm into the depth of the glass. The tin concentration on the tin side of the float glass varies between 2 % and 5 % [3]. Most of the tin on the tin side is in the oxidation state Sn^{2+} [6]. Tin reacts with silver ions according to the following reaction:

$$Sn^{2+} + 2\,Ag^{+} = Sn^{4+} + 2\,Ag^{0}$$

Tin ions react with silver ions to form silver colloids. These colloids absorb radiation in the range of 400-420 nm [7]. The reducing atmosphere in the furnace helps to oxidise silver. The pre-treatment of the glass in a reducing atmosphere helps to reduce the tin in the near surface of the glass, which results in more silver being reduced during the heat treatment of the silvered sample. On the contrary, pre-treatment in an oxidising atmosphere leads to the oxidation of tin to the Sn^{4+} state. This pre-treatment results in less Sn^{2+} being available for the silver diffusion in the thermal process [7].

The accumulation of contaminants on the glass surface is not a primary consequence of low temperature annealing. Electron or ion beam effects, such as increased diffusion [3] or desorption [8], could prevent the detection of impurities at the interface. It has been discussed that impurities containing silver on their surface may not be visible to the naked eye prior to the thermal process. The surface of the glass may be clean, but even a weak layer of dirt on the tin side of the glass will lead to silver diffusion and silver nucleation in the glass [8]. Contamination of the tin surface of the glass can occur in the processes where they are applied to the glass coating. This contamination can be difficult to detect in the next process, as it can be very small layers of nanometres to millimetres, depending on whether the silver-containing impurities have agglomerated before contaminating the glass. However, float glass does not appear to contribute to the apparent accumulation of impurities on its surface during the annealing process.

The occurrence of silver agglomeration during annealing will lead to an increase in the diffusion distance. The rate of sputtering through the interface is constant and equivalent to the rate through pure silver [9].

Mild glass annealing without contamination does not significantly change the characteristics of the silver-glass interface [10].

The diffusion behaviour of silver ions on the tin and air side of float glass is different. The silver concentration profile for the underside of the glass is significantly suppressed near to the area where the peak in the tin concentration profile is located. This behaviour is not observed on the air side of the float glass. The behaviour is attributed to the ongoing chemical reactions between the Ag^+ and Sn^{2+}. The optical absorption at 400 nm is different, due to the resonance of the surface plasmon in the Ag^0 crystals, which is visible in Figure 1 [1].

As mentioned above, most of the tin near the bottom surface exists as Sn^{2+} [12]. The depth of the suppression in the Ag concentration profile is strongly dependent on the position of the peak in the Sn depth profile, which causes discolouration because the nucleation and growth process of Ag colloids is strongly influenced by the depth of the tin profile [11]. The control of the depth profile of tin (Sn^{2+}) is critical for controlling the colour caused by the nucleation of silver in the depth of the glass. The depth of the tin in the glass surface is determined by the production conditions on the float line, the time of contact of the glass with the tin in the tin bath is important, as well as the temperature profile and the occurrence of impurities in the atmosphere during the treatment [13]. The precise control of the process conditions is necessary to control colour.

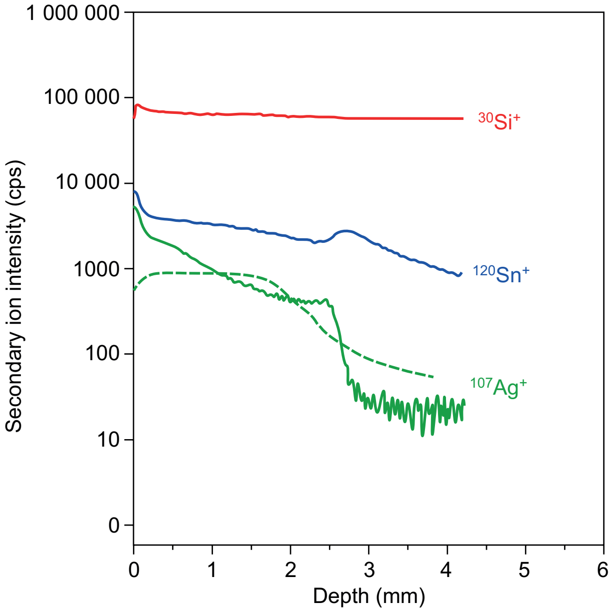

Figure 1. SIMS depth profile of $^{107}Ag^+$ for the top and bottom face of an Ag-diffused soda–lime–silica float glass [11].

Silver-based coated glass is a high value product that many customers in the automotive industry require. Silver-based glass combines the properties of heating with the properties of reflection selectively for infrared radiation. This product provides the driver with greater comfort in winter and summer. When the internal heat energy tries to escape into the colder outdoor area during the winter, the low emissivity layer reflects the radiation back inside and reduces the heat loss by radiation through the glass. Typical products using silver-based coatings are windshields in the automotive industry [14]. When the emissivity of the window coating is low, the window coating is called a low emissivity coating. Low emissivity coatings have been developed to minimise the amount of ultraviolet and infrared light that can pass through the glass without reducing the amount of visible light passing through the glass. There are two main types of low emissivity coating processes – a pyrolytic low emission coating sometimes referred to as a hard coating and magnetron sputtering vacuum deposition (MSVD), or “soft coating”.

In the MSVD process, the coating is applied off-line to pre-cut glass in vacuum chambers at room temperature. The low emissivity pyrolytic coating for single pane glass achieves an emissivity of 20 %, while silver-based spray coatings can achieve an emissivity of 2-8 %. 90 % of the current market is made up of low emissivity products, as it combines several of the benefits mentioned earlier. [15]. The history of the production of low-emissivity coatings is short, but, in recent years, the development of the production of glass with this coating is on the rise. The electrical and optical properties of a silver-containing thin film strongly depend on its microstructure, such as the crystallite size, grain size, grain boundaries, and surface roughness. The electrical and optical properties also depend on the very structure of the other dielectric layers, which are, in the given coating, used as supporting layers ensuring optimal coating properties. The aim of the current research is focused on the microstructure of thin silver in order to achieve optimal optical parameters and heating parameters [16].

The use of a germ layer is standard in deposition techniques. The aim of the seed layer is to improve the optical and mechanical properties of the coating, which is achieved by supporting the microstructure of the thin film. The ZnO seed layer can be used to increase the size of the silver crystallites in the coating. By changing the size of the silver crystallites, like by changing the size of the silver grain, its absorption is reduced and its resistivity is reduced. Crystallising silver (111) at the top of the basal plane ZnO (002) leads to a lower resistivity value than the polycrystalline silver located at the top of zinc stannate. ZnO is an easily crystallising material at room temperature even at thicknesses above 5 nanometres. The places of the ZnO grid are in the corners and in the centre of the hexagon. The three silver atoms at the alternating quadruple hollow sites form the base cell (111) of the silver plane with a 2.6 % lattice mismatch between the ZnO and Ag layers, so that the crystallised ZnO lattice promotes the silver growth in the (111) direction [17; 18].

The silver film is under an unstable and soft material under an oxygen plasma. The silver film easily oxidises into silver ions (Ag^+), allowing silver to diffuse into adjacent layers. The oxidation of silver and its diffusion into adjacent layers results in the deterioration of the optical properties of the coated glass. In addition, the conductivity of the electric current of the coated glass deteriorates.

The top layer of the coating consists of materials such as TiO_2, SiO_2 or ZnO. The quality of the low-emission coating is mainly determined by the crystalline silver, the presence of a blocking layer (called a blocker), which blocks the oxidation of silver, is necessary. The blocker is made up of titanium, for example. The blocker must not be too thin to effectively block the oxidation of the silver from the adjacent layer. Increasing the thickness of the blocker layer leads to a slight increase in the emissivity of the coated glass. The typical thickness of the blocking layer is 10 nm. The so-called seed layer serves as a basis for the growth of silver crystals, which is most often formed by zinc oxide. The typical seed layer thickness is 15-20 nm. The intermediate layer, which is located between the seed layer and the blocker layer, or between the seed layer and the glass, is formed by oxides of tin and zinc (so-called zinc stannate). This layer can have a thickness of several tens of nm. The total thickness of the coating with two layers of silver can be 150-250 nm. For layers containing multiple layers of silver, the typical coating thickness is 250-350 nm (Figures 2-3).

Zinc stannate – zinc oxide – silver coating layers can be designated a building block for low-emissivity multi-layer coatings. The introduction of two or three of these blocks results in a coating with low emissivity, therefore, with higher selectivity between infrared (IR) and visible light. A typical coating structure with three blocks containing silver is shown in Figure 3 [17].

Silver-based coating glass is used in the automotive industry to produce heated, low emissivity coated windshields. When we talk about the advantages of a silver-plated windshield compared to a standard windshield, we can mention the heating power caused by the current distribution between the coating and the busbars. The possibility of heating allows defrosting and demisting

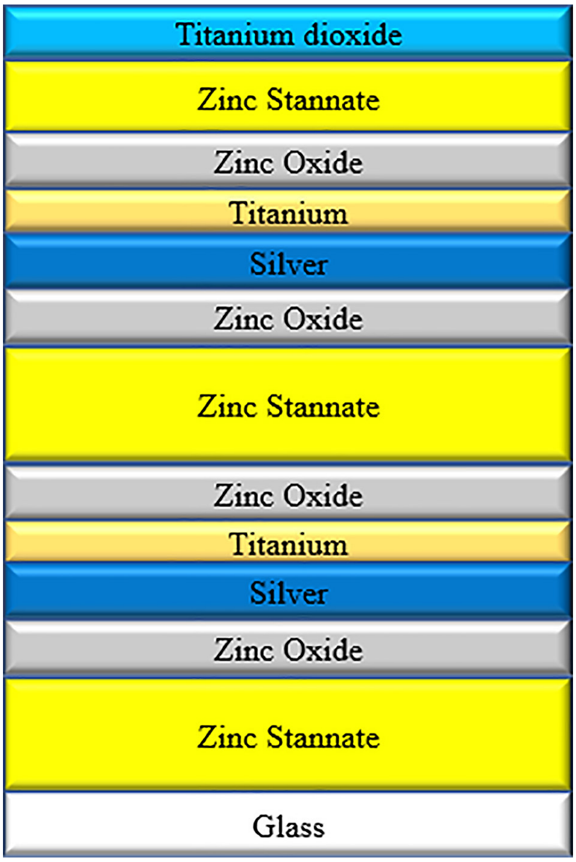

Figure 2. Example of the silver-based coating composition.

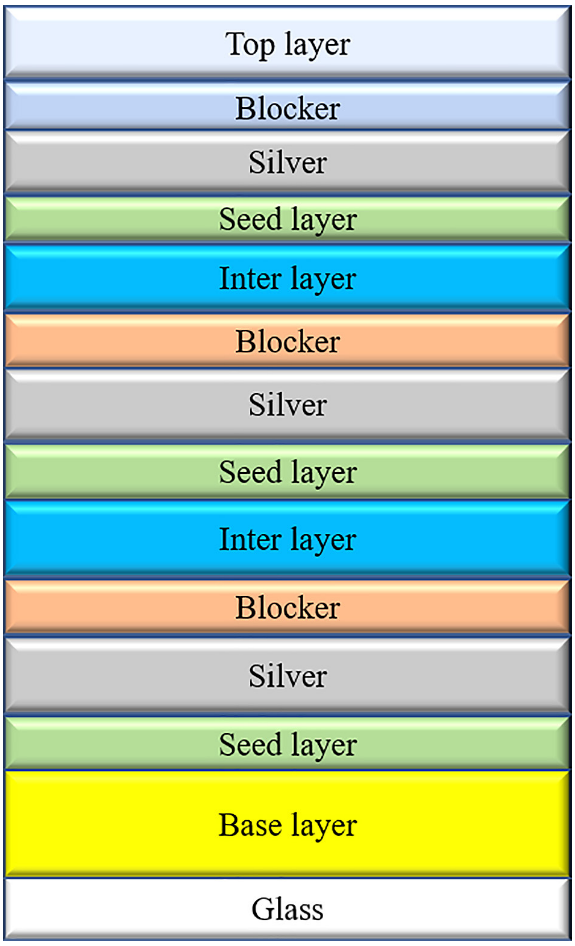

Figure 3. Example of the silver-based coating composition.

of the windshield. The heated coated windshield is able to control and modulate the amount of radiation coming into and out of the car. This product has been very popular in the automotive industry for the last 20 years and its popularity is still growing. In this article, we will primarily focus on the application of silver paint to car windshields [18].

The production of a heated coated windscreen begins on a float furnace (Figure 4). For the production of glass used for automotive glass, a tin bath float process is used [19]. Thicknesses of float flat glass in the range of 0.5 to 20 mm were produced for various applications of the given float glass. The homogeneous glass melt is poured onto a bath of molten tin under optimal process conditions and forms a floating strip. The floating of glass by tin is enabled by different densities of the glass and molten tin (the density of the molten tin is about three times greater than the density of the glass). As the molten glass moves through the tin bath, the temperature gradually decreases from 1100 °C to about 650 °C, where the glass sheet can be bridged from the tin bath on a cylinder in an annealing furnace. The glass strip is removed from the bath by rollers at a controlled speed. The difference between the melt flow rate and the drawing speed of the cylinder allows the formation of glass sheets of different thicknesses. The product of the float process is a continuous glass tape. This tape is basified with SO_3 gas and then cut into glass sheets. These sheets are then palletised so that they are ready for transport to the next process [11].

A coating is applied to the float glass in another process – the coating sputtering process. Sputtering is the process of coating a substrate with material removed from a target by sputtering. By sputtering, a coating of a defined material located on a solid target is applied to the passing glass by ion bombardment. Magnetically limited plasma creates ions above the surface of the target, i.e., the material that is sputtered on the passing glass (Figure 5) [15].

A coater is a machine that applies a thin layer to the passing glass. The application process is called the whole coating process from placing the glass on the conveyor to removing it back (Figure 6).

The glass sheet is robotically loaded onto the line by a manipulator. The robot grabs the glass from the pallet with a suction cup and places it on the line. Washing the glass before the coating is a critical operation. The glass surface must be sufficiently clean, free of solid or liquid impurities, otherwise any contamination will be covered during the coating process and a defect will occur (the most common defect is the peeling of the coating). We use intensive scrubbing of the glass with brushes,

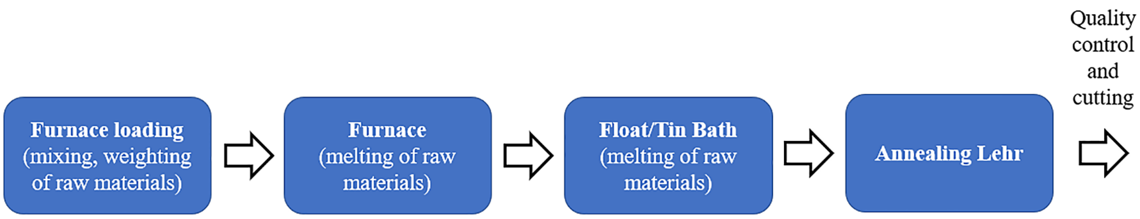

Figure 4. Schematic of a float batch production line.

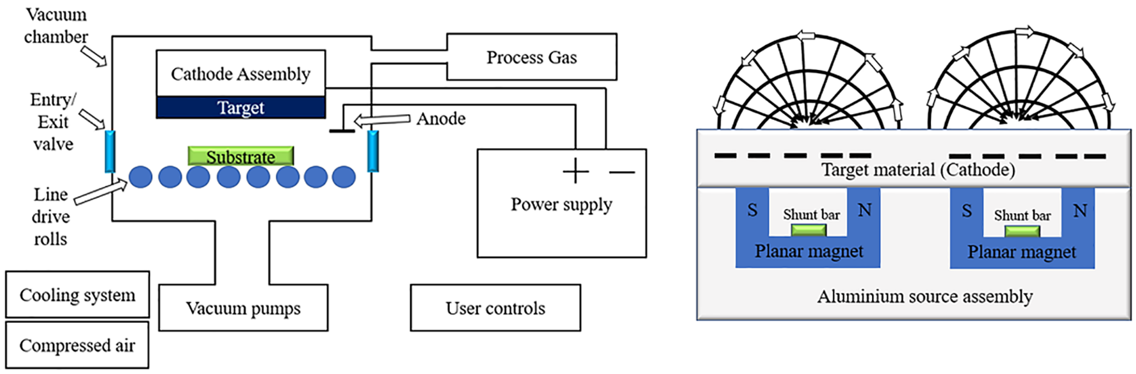

Figure 5. Sputter coating machine design and magnetron construction.

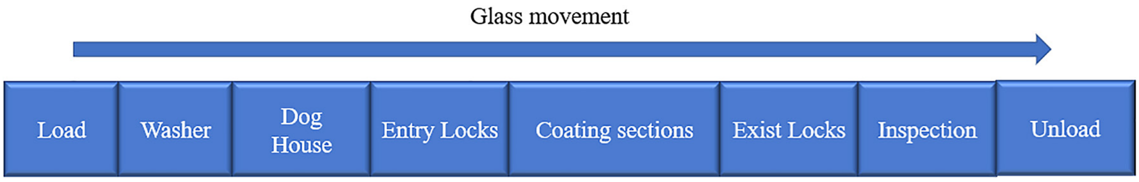

Figure 6. Typical coating process block diagram.

rinsing and drying using an air knife. Washing is performed with low conductivity water below 0.5 $\mu S \cdot cm^{-1}$ at a temperature between 15 °C and 20 °C. The washing water is without any chemical additives. Regular maintenance of the washing machine must be performed once every 2 to 3 weeks. The washing machine is cleaned with hydrogen peroxide to get rid of mould or its spores, and high-pressure water jets are used to clean the construction of the washing machine. Dirt from the glass surface is removed by positive pressure cleaning in the area of the line, which is called the "kennel". The entrance lock system consists of three chambers: the lock, retainer and bumper. The conveyor transports the glass to the vacuum coating chamber. The entrance lock system cycles between atmospheric pressure and vacuum (101 325 Pa to 2 Pa). It consists of a chamber with slit valves to maintain the vacuum, rollers to transport the glass, pumps to create the vacuum and vent valves to regain atmospheric pressure. The pump cycle with the inlet lock and inlet space is under vacuum (< 2 Pa). Diffusion pumps and cryogenic pumps are used for pumping. This is where the glass can be stopped before it enters the chambers where the final coating (coating chambers) is applied to the glass.

A high vacuum is always achieved in the vacuum chambers. Diffusion pumps are again used for pumping. The glass continuously moves through the chambers with the help of rollers. The aim is to prevent gaps from occurring in the glass so that the material is not applied to the rollers on which the glass moves and, thus, dirt is imprinted on the side of the glass which is in contact with these rollers. The tin side of the float glass is in contact with the rollers during the coating process on the air side of the float glass. The composition of the coating layers depends on the order in which the materials are applied to the glass in the process, i.e., the first applied layer will be in contact with the air side of the glass, the second applied layer will be in contact with the first applied layer and the layer to be applied in the next step, etc. The length of the coating line depends on the composition of the coating itself – for example, the triple silver coating used for automotive purposes is much longer than the single silver coating used for architectural purposes (Figure 7).

The exit locks consist of three chambers – the buffer chamber, hold chamber and lock chamber. The continuous flow of glass is ensured by the inlet closure system. The coated glass is inspected online for defects and its colour. The rejected glasses are marked and automatically discarded directly within the line [20-21].

As a rule, the coated sheet is transported to a line that is able to process the given glass coating into the form of an automobile windshield. On a given line that processes glass into the shape of a car windshield, the glass is first loaded onto the line. In subsequent processes, the glass is cut to the required dimensions, ground, and printed with black printing ink. The printed glass is then bent most often on a gravity bending furnace. Gravity bending is best used for short series because many different types of moulds can be used in the process at the same time. This makes it the best bending process for car glass manufacturers, as only one mould is needed for a short series. In the past, shaping was difficult because the heat only came from above. Now with the latest technology, concentrated total heating with power control and double-controlled moulds with triggers allow for much more precise shape control, leading to a better final quality (Figure 8) [22].

The gravity bending technology, in which glass sheets are bent in pairs on moulds, is used to process coated glass. Heat is applied through this process and the largest number of defects are observed after this particular step in the process – the bending operation. By applying heat to a silver coated glass sheet, diffusion processes begin and ions begin to migrate when the glass temperature exceeds 270 °C [23]. The presence of silver-containing contamination on the tin side of the glass leads to the diffusion of silver ions from the contamination into the glass surface and to the formation of silver nuclei, as previously described in detail [14].

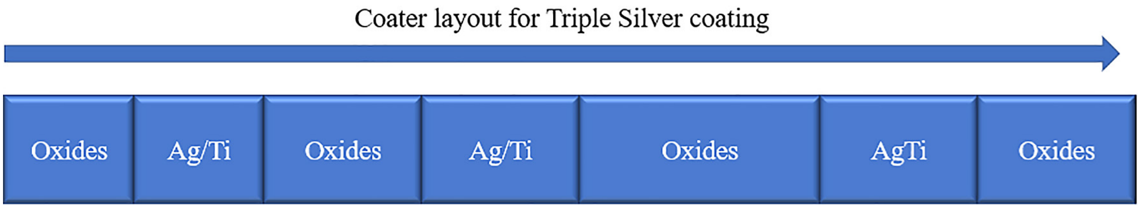

Figure 7. Coater layout for the triple silver coating production.

Figure 8. Schematic of the gravity bending technology.

Once the glass is bent, it enters the post-processing line. Before assembling the interlayer glasses, the glasses are washed again with water. The purity of the water in this intermediate step plays a key role in achieving optimal adhesion between the inner glass, the polyvinyl butyral (PVB) film and the outer glass. The inner and outer glass with PVB is prepressed in a press furnace. In the next step, the glass enters the autoclave. At the end of the autoclave cycle, the PVB comes into full contact with the glass. Then the glass is checked for visual defects and then sent to another operation, where the glass is washed again and other plastic and other parts are applied to it, most often by gluing to the glass using adhesives [22].

EXPERIMENTAL

Preparation of samples

Commercially available float glass samples were subjected to heating with a powder that contained a mixture of oxides that traditionally form the coating layers. The composition of the glass powder is 50 wt. % ZnO and 50 wt. % of Ag_2O. The glass was placed in a melting laboratory furnace with the air side toward the furnace construction parts and the powder sample was deposited on the tin side of the float glass. The samples were heated up to 650 °C, so above the glass transition temperature of the given glass (Figure 9-10). This temperature is the temperature at which the silver is activated and, thus, allows the impurity components to diffuse into the glass.

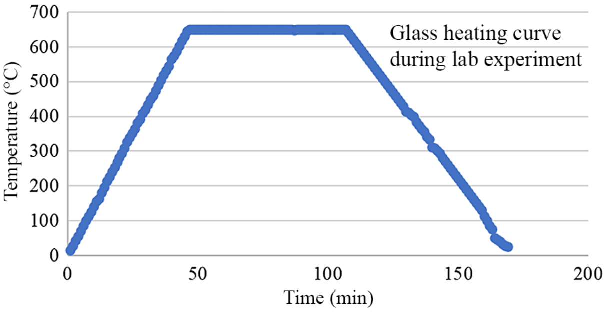

Figure 9. Optical microscopy of the defect.

The defect created on the tin face of the float glass was analysed further (Figure 11).

Laboratory analyses – microscopy

The coating defect is analysed using several laboratory techniques to obtain the most detailed information about the defect. The VK-X3000 Series 3D surface profilometer uses a triple scanning approach, using a laser confocal method, variable focus method or white light interferometry method, which ensures the highly accurate measurement and analysis of various objects. The maximum resolution of 500 nm ensures the accurate measurement of any shape deviations in the nanometre range.

Laboratory analyses – Raman spectroscopy

Raman spectra were measured with a Raman dispersion spectrometer from Thermo Scientific – a DXR Microscope model equipped with an Olympus confocal microscope. A diode-excited Nd: YAG laser with a wavelength of 532 nm and a power input of 10 mW served as the excitation source. A grid of 900 scratches / mm was used for the measurement. A multi-channel thermoelectrically cooled CCD camera served as a detector. The samples were measured at 50× magnification. To exclude the thermal degradation of the sample, measurements were made at a power of 2 mW, a measurement time of 10 s and with spectrum accumulation. The optical microscope analysis was performed by a Keyence optical microscope VHX-6000 Series with large depth of field with a 3D analysis capability.

Laboratory analyses – X-ray fluorescence

A fully automatic sequential XRF spectrometer for qualitative and quantitative elemental analysis of up to 83 elements (B–C O–U) ranging from ppm to 100 % was used for the XRF data measurement. It consists of an Rh lamp, a 4-kW generator, 4 collimators, 6 crystals (AX 20, TLAP, PET, Ge 111, LiF 200, LiF 220), and 2 detectors – proportional and scintillation. The non-standard analyses were conducted using UNIQUANT 4 software, the analyses using calibration curves were conducted using Winxrf software.

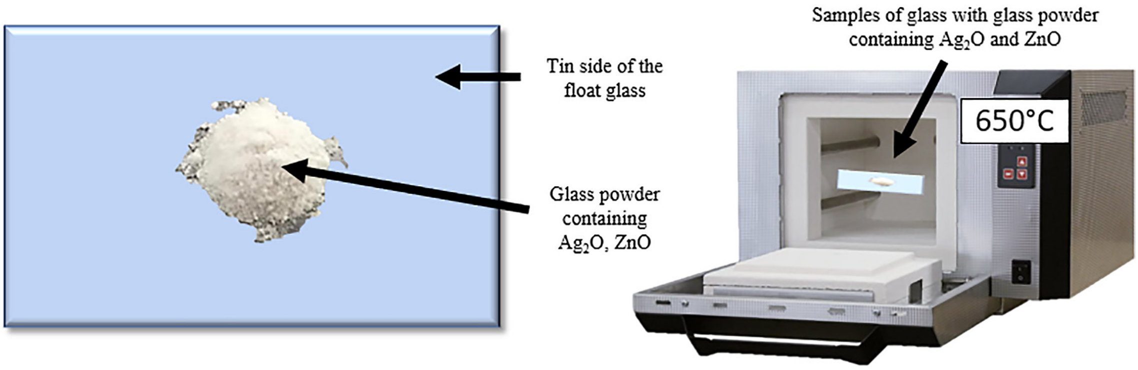

Figure 10. Optical microscopy of the defect.

Laboratory analyses – XPS analysis

An XPS analysis device was used for the analysis. The machine consists of an analysis chamber, a preparation chamber, an inlet chamber combined with an exposure chamber. An evaporator and an ion cannon are connected to the preparation chamber. In addition to a hemispherical electron detector equipped with 5 chaneltrons, the analytical chamber has another ion cannon, a secondary electron analyser, a monochromatic X-ray source (1486.7 eV), a focusable electron source for the Auger analysis, a low-energy electron source to compensate for the sample charging and low energy electron diffraction (LEED) and dual X-rays source (Al/Mg). The analysis takes place in a UHV vacuum at pressures of the order of 1-10 mbar. Analyses can be performed at elevated temperatures (up to 400 °C) as well as at low temperatures (temperatures close to liquid nitrogen). The basis is an electron microscope (SEM) with a Schottky cathode as a compromise between the ultimate resolution (1 nm) and the maximum current (200 nA). The microscope is equipped with two secondary electron (SE) detectors, one of which is in the sample chamber and the other is in the column, and a reflected electron detector (BSE). A combination of excellent lateral resolution with the possibility of allowing smooth magnification, a computational table, and reproducibility of the movement in the sample chamber with good sample orientation and site selection based on a topographic or phase contrast. The electron tube is supplemented by ion optics with a Ga source, which it offers according to the selected mode sample dedusting, ion microscopy with detection of SE or secondary ions (SIs) with a resolution of up to 2.5 nm, or a negative charge compensation on the sample surface. The microscopic characterisation is completed with a simple optical microscope that is part of the Raman spectroscopy (RS).

Laboratory analyses – SEM-EDX analysis

A representative sample is examined by SEM-EDX analysis. SEM provides detailed, high-resolution images of the sample by scanning a focused electron beam across the surface and detecting a secondary or backscattered electron signal. An energy dispersive X-ray analyser (EDX) is also used to provide element identification and quantitative composition information. A Hitachi SU8230 Regulus Ultra High-Resolution Field Emission SEM was used for the measurement. The Hitachi device has an image resolution of 0.6 nm at 15 kV with a magnification range of 20× to 2 000 000×.

Materials

The laboratory float glass subjected to the Ag_2O and ZnO powder was used for the analysis. These two elements are the basic components of silver-based coatings used for architectural and automotive purposes.

RESULTS

Laboratory analyses – microscopy

Confocal microscopy was used to analyse the defect. The observed defect has a diameter of 1.73 mm. The shape of the defect is inconsistent, the defect is not bounded and is composed of one large defect and several other smaller defects in the vicinity of the main defect. The defect is created in the area where we subjected the glass to the powder substance (Figure 11). We can observe different colouration in different areas of the tin glass surface where the glass has been in the contact with the Ag_2O and ZnO powder.

The 3-D measurements showed that the defect protrudes from the glass surface, its shape is peeled. The defect is probably material that is located on the glass surface having a possible effect on the structure of the glass surface. The defect has a golden colour in its centre, outside the main defect there are smaller defects of a metallic colour. The different colours of the defect and the shape of the defect indicate a possible chemical reaction taking place at the defect site (Figure 12).

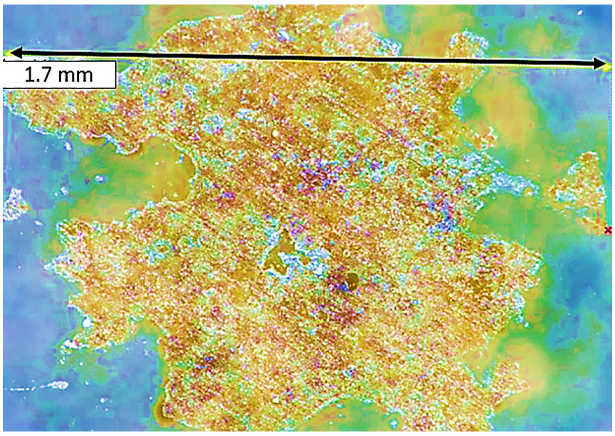

Figure 11. Optical microscopy of the defect.

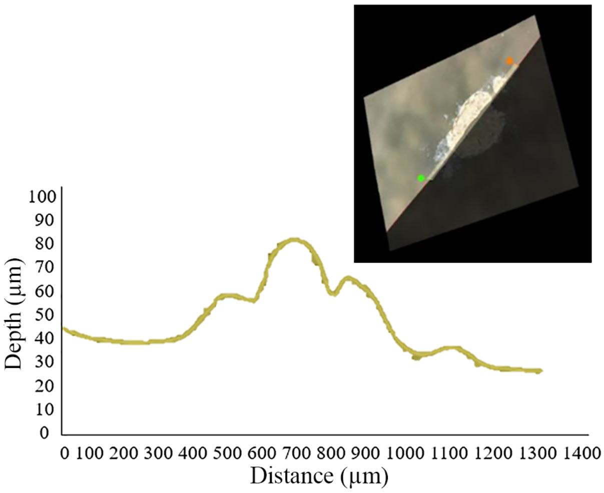

Figure 12. Confocal microscopy – depth profiling of the defect.

Laboratory analyses – Raman spectroscopy

The defect area was cleaned by isopropyl alcohol before its analysis by Raman spectroscopy to remove the peeling material. The analysis concentrates only on the areas where the interaction of the powder with the glass is evident. Raman spectroscopy is used to analyse the defect composition from the point of view of its organic composition. The spectra are measured at different defect sites. There are visible peaks in 237 cm^{-1}, 347 cm^{-1}, 471 cm^{-1}, 563 cm^{-1}, 641 cm^{-1}. The spectrum is then compared with the spectrum of SnO_2 and ZnO. SnO_2 is on the tin side naturally due to the process of floating the glass in a tin bath. The presence of ZnO refers to an impurity on the glass surface able to react with the tin glass surface. Zn^{2+} ions seem to be diffused in the glass surface (Figures 13-14).

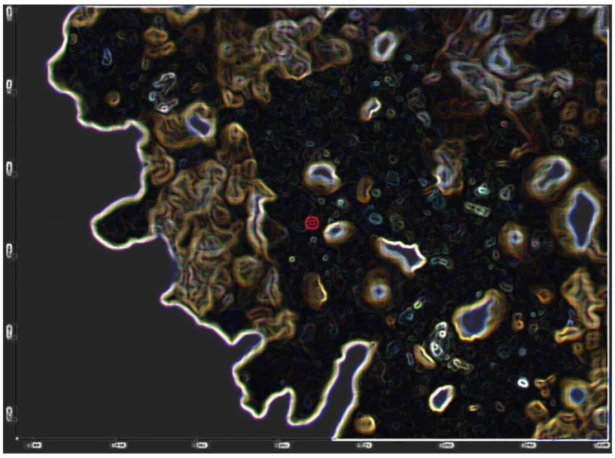

Figure 13. Optical microscopy – the appearance of the defect.

Laboratory analyses – X-ray fluorescence

X-ray fluorescence analysis is used to map the glass composition at the defect site and outside the defect area. The result is a comparison of the composition in both places – in the area of the defect and in the area out of the defect. We can observe a higher amount of SiO_2, Fe_2O_3, Ag_2O, K_2O, SO_3 and ZnO in the defect area (Figure 15). We can observe a negligible amount of Ag in the defect area using X-ray fluorescence mapping, otherwise, we can observe a significant amount of Fe and Zn (Figure 16). We attribute iron to the contamination of the powder during its production or preparation in the laboratory.

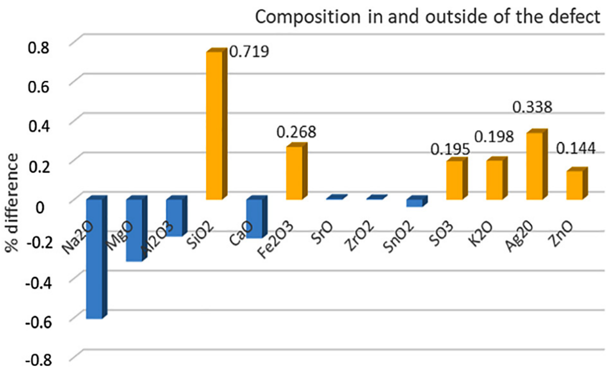

Figure 15. X-ray fluorescence analysis – elementary composition in the area of the defect.

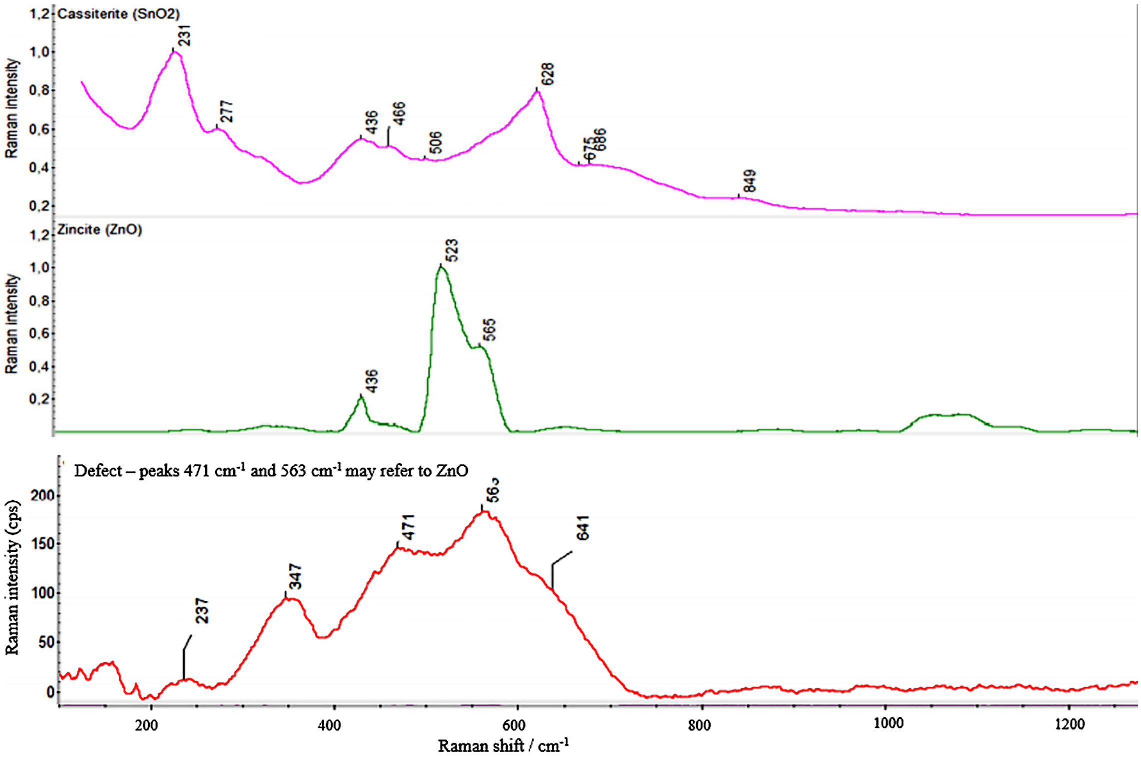

Figure 14. Raman spectroscopy analysis of the defect.

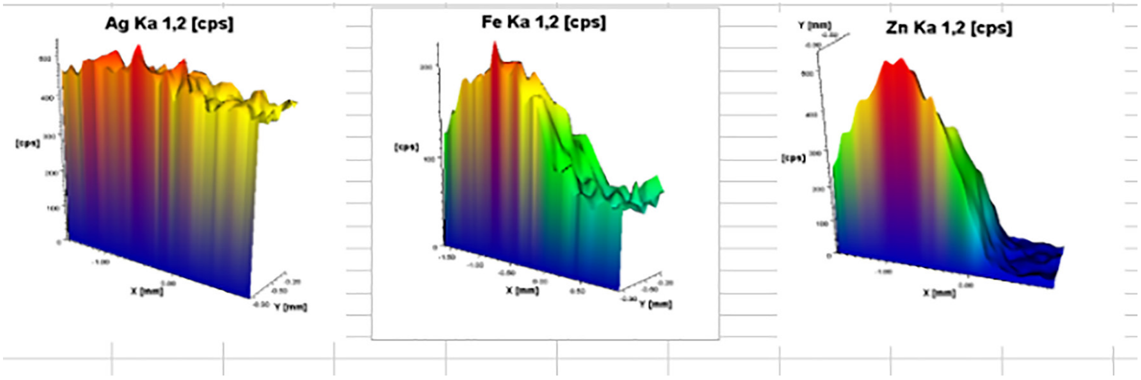

Figure 16. X-ray fluorescence mapping of the silver, iron, and zinc.

Laboratory analyses – XPS analysis

XPS analysis is used to analyse the depth profile over time. At 5 minutes, zinc oxide (1022.37 eV), the atomic weight (5.04 %), silver oxide (368.12 eV, 374.18 eV), and the atomic weight (6.53 %) were detected in the defected area (Figures 17 and 18).

The XPS analysis was conducted for 2 hours to analyse the surface concentration profile of the Zn and Ag elements on the tin side of the float glass. The surface profiles are depicted in Figures 5-6. During longer XPS analysis times, the concentration profile of the zinc and silver in the glass showing a maximum at different depths of the glass was detected. Zinc ions were obviously not able to diffuse into the deeper layers of the glasses and show a maximum concentration after 10 minutes of dedusting, namely 6.03 % atomic weight, while silver shows a maximum concentration at 40 minutes of dedusting, namely 8.1 % atomic weight.

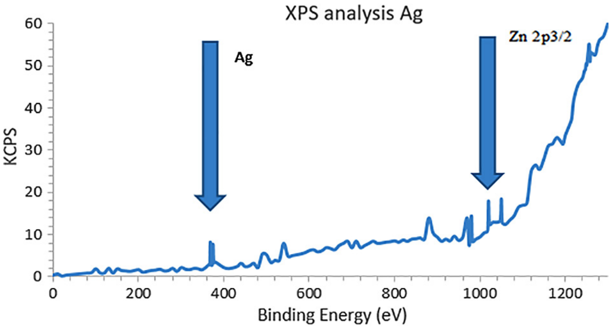

Figure 17. XPS analysis in the defect area showing the presence of Ag and Zn.

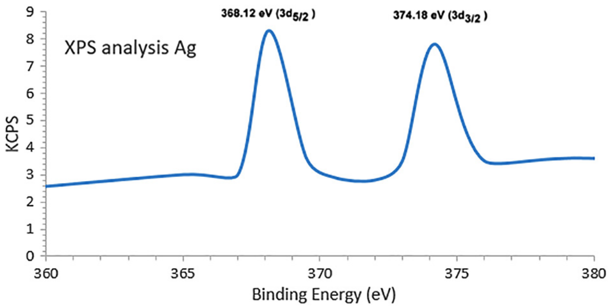

Figure 18. XPS analysis of the silver.

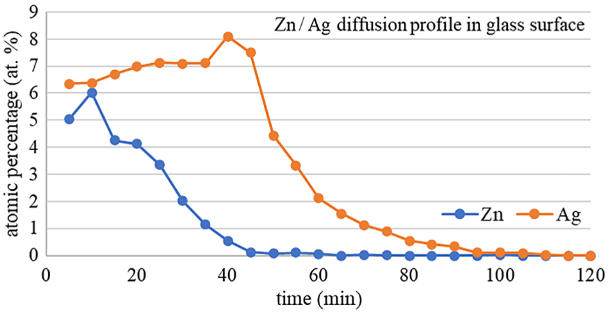

Figure 19. Diffusion profile of the Zn / Ag on the tin side of the float glass.

Laboratory analyses – SEM-EDX analysis

The defect was further analysed by SEM-EDX analysis. The defect is evidently cracked in various places, and on the microscope image, the defect appeared differently than in the case of the previous analyses. The reaction between the glass and the powder on the surface of the glass is clearly visible. The defect appears as an impurity applied in the process to the glass, which subsequently reacts with the glass at higher temperatures to form grains in the glass, causing the apparent discolouration of the defect site. The increased Ag content is analysed at the defect site. The probable mechanism reveals the diffusion of Ag$^+$ ions from the impurity, with Ag^0 nucleating at different depths of the glass. These Ag^0 grains appear golden. The presence of elements, such as zinc (34.97 %), tin (24.62 %), silver (12.05 %), titanium (4.77 %), was detected at the defect site. We attributed titanium to the contamination of the powder during its production or preparation in the laboratory. All these elements are found in the coating layers (Figures 19-20, Table 1). Thus, the probable cause is the interaction of the powder with the tin side of the float glass.

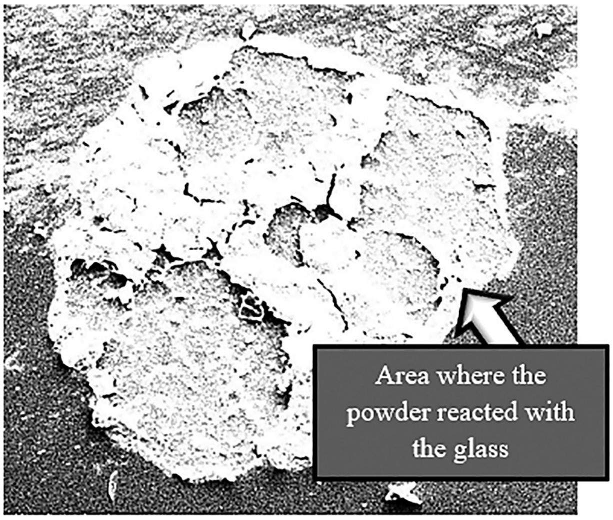

Figure 20. SEM-EDX analysis of the defect – microscopic picture.

Table 1. SEM-EDX analysis of the defect.

Element	Mass (%)
Oxygen	16.42
Silicon	2.89
Calcium	1.45
Titanium	4.77
Iron	2.83
Zinc	34.27
Silver	12.05
Tin	24.62

DISCUSSION

The most common defect on the tin side of the glass was simulated in the laboratory by the heating experiment with the float glass in which tin side was subjected to the silver oxide and zinc oxide powder. The created defect was subjected to several analyses in order to discuss the mechanism of the defect and its possible origin. The microscopic analyses revealed that the defect consisted of one large defect and several smaller contiguous ones, with the size of the main defect being 1734 micrometres for the analysed glass sample with the defect. The size of the surrounding smaller defects ranges from tens to hundreds of micrometres. The defect has an irregular shape that protrudes above the glass surface. Above the surface of the glass, a kind of peel of foreign material is visible. This peel, as well as the shape of the defect, is attributed to the reaction of the glass with the powder. The defect is evidently coloured under the microscope, the centre of the defect being golden and the area around the defect being metallic in colour. This defect is very easy to simulate in the laboratory when a powder containing silver ions is in contact with glass. When processing coated glass, great caution is necessary and an effort to maximally avoid contact of the material containing silver ions with the reactive tin side of the glass, especially if the given glass is heated in the following process to temperatures exceeding 390 °C, i.e., temperatures at which it is activated diffusion process of silver ions into glass. The defect was first studied by Raman spectroscopy to detect any possible organic pollution. Tin and zinc oxides were detected at the defect site (SnO_2, ZnO).

The X-Ray fluorescence method confirmed the presence of ZnO from the previous Raman spectroscopy analysis. Oxides of SiO_2, Fe_2O_3, SO_3, K_2O, Ag_2O and ZnO were detected at the defect site. Based on the X-ray analysis, other oxides consisted of SiO_2 (+ 0.749 % of the original composition), Fe_2O_3 (+ 0.268 % of the original composition), SO_3 (+ 0.195 % of the original composition), K_2O (+ 0.198 % of the original composition), Ag_2O (+ 0.338 % compared to original loading), ZnO (+ 0.144 % compared to original composition). We attributed the presence of SiO_2 and K_2O to the evidence of the ongoing chemical reaction between the glass surface and the given defect on the glass surface. We attributed the presence of SO_3 to the process of glass decalcification in the float production process. The origin of ZnO and Ag_2O is attributed to the reaction of the powder with the glass.

The XPS analysis confirmed the previous Raman spectroscopy (the presence of ZnO) and XRF findings (the presence of ZnO and Ag_2O). After 5 minutes, only zinc oxide (1022.37 eV) with an atomic weight (7.04 %) were detected in the defect area and silver oxide (368.12 eV, 374.18 eV) with an atomic weight (6.53 %) were detected in the damaged area. During longer XPS analysis times, the concentration profile of zinc and silver in the glass showed a maximum at different glass depths was detected. Zinc ions were obviously not able to diffuse into the deeper layers of the glasses and show a maximum concentration after 10 minutes of dedusting, specifically 6.03 % atomic weight, while silver shows a maximum concentration at 40 minutes of dedusting, specifically 8.1 % atomic weight.

The last SEM-EDX analysis indicated the presence of other elements. We detected zinc, tin, silver and titanium at different atomic %s. The presence of zinc and silver is subjected to the powder to which the tin side of the float glass has been exposed. The presence of tin is attributed to the float glass and we consider titanium as the contamination at the end. After reheating above the glass transition temperature of the glass, there is an intense diffusion of silver ions into the glass (Ag^+) and the subsequent nucleation of Ag^0 grains at different glass depths. Depending on the amount of pre-reacted silver, the defect area turns gold. In places where silver does not diffuse into the glass, the original metallic colour remains. As part of the float glass process, the tin side must be kept free of silver particles that may interact with the tin side of the float glass and cause the intensive colouration of the float glass. This aspect failure means glass quality deterioration.

CONCLUSIONS

In the case of the presence of contamination on the tin side of the glass, the thermal heating of the glass causes the diffusion of silver ions to a depth close to the glass surface and its subsequent nucleation. Ag^0, which has a typical orange colour, is formed. Diffusion occurs due to the presence of silver on the tin side of the glass by the diffusion process. Silver ions diffuse into the glass, while the most common Sn^{2+} ions diffuse from the glass on the surface. The chemical analysis confirmed the presence of silver and zinc particles diffused to the glass. The defect was simulated in the laboratory conditions with the glass exposure to the powder consisting of the silver oxide and zinc oxide. The glass was heated to 650 °C and exposed to this temperature for 1 hour. It was then cooled again in a controlled manner and the defect was analysed by laboratory techniques. The confocal microscopy detected different colouration in different areas of the tin glass surface where the glass had been in the contact with the Ag$_2$O and ZnO powder. The shape of the defect was determined as being irregular. Raman spectroscopy detected the presence of ZnO. The presence of ZnO refers to an impurity on the glass surface able to react with the tin glass surface. Zn^{2+} ions seem to be diffused in the glass surface. The X-ray fluorescence analysis revealed a higher amount of SiO$_2$, Fe$_2$O$_3$, Ag$_2$O, K$_2$O, SO$_3$ and ZnO in the defect area (Figure 1). Only a negligible amount of Ag in the defect area was found. The SEM-EDX analysis unveiled the presence of elements such as zinc (34.97 %), tin (24.62 %), silver (12.05 %), titanium (4.77 %) at the defect site. We attributed the titanium to the contamination of the powder during its production or preparation in the laboratory. The probable cause is the interaction of the powder with the tin side of the float glass.

The concentration profiles of zinc and silver in the glass were measured by XPS. The result of the XPS was the concentration profile of zinc and silver in the exposed location. A concentration profile of zinc and silver in the glass showing a maximum at different glass depths was detected. Zinc ions show a maximum concentration after 10 minutes of dedusting, specifically 6.03 % atomic weight, while silver shows a maximum concentration at 40 minutes of dedusting, specifically 8.1 % atomic weight.

Depending on the amount of pre-reacted silver, the defect area turns gold. In places where silver does not diffuse into the glass, the original metallic colour remains. As a result, the slightest contaminant on the tin side of the glass containing reactive ions can (especially silver ions) degrade the quality of the glass.

REFERENCES

1. Bamford C. R. (1977): Colour generation and control in glass. *Elsevier Scientific Publishing Co., Amsterdam and New York*, 25-41. Doi: 10.1002/col.5080030317
2. Stookey S. D. (1949):, Coloration of glass by gold, silver, and copper. *Journal of the American Ceramic Society*, 8, 246-249. Doi: 10.1111/j.1151-2916.1949.tb18957.x
3. Shelby J. E., Vitko J. (1982): Colloidal silver formation at the surface of the gloat glass. *Journal of Non-Crystalline solids*, *50*(1), 107-117. Doi: 10.1016/0022-3093(82)90204-6
4. Puche-Roig A. (2008): Float glass colouring by ion exchange, *Journal of Cultural Heritage*, *9*, 129-133. Doi: 10.1016/j.culher.2008.08.006
5. Feng, C. H., Chu M. W., Ku, C. H. (2020): Ag-diffusion inhibition mechanism in SiO -added glass-ceramics for 5G antenna applications. *Ceramics International, 46*(15), 24083–24090. Doi: 10.1016/j.ceramint.2020.06.186
6. Hench L. L., Clark D.E. (1978): Physical chemistry of glass surfaces. *Journal of Non-Crystalline solids, 28*(1), 83-105. Doi: 10.1016/0022-3093(78)90077-7
7. Suyal G., Mennig M., Schmidt H. (2004): Effect of Glass Substrates on the Formation of gold-silver Colloids in Nanocomposite Thin Films. *Journal of sol-gel science and technology, 29*, 11-18. Doi: 10.1023/B:JSST.0000016132.87265.f9
8. Mehrer H. (2016): Diffusion and Ion Conduction in Cation-Conducting Oxide Glasses, *Diffusion Foundations, 6*, 59-106. Doi: 10.4028/www.scientific.net/DF.6.59
9. Hayashi Y., Matumoto K., Kudo M. (2001): The Diffusion Mechanism of tin into Glass during the Float Process, *Hyomen Kagaku, 22*(7), 412-418. Doi: 10.1380/jsssj.22.412
10. Takeda S., Kiyoshi Y., Kiyoshi M. (2000): Coloration due to colloidal Ag particles formed in float glass. *Journal of Non-Crystalline Solids, 265*(1), 133-142. Doi: 10.1016/S0022-3093(99)00711-5
11. Bastasz R. (1980): Auger analysis of silver-glass interfaces.*Solar Energy Materials, 3*(1-2), 169-176. Doi: 10.1016/0165-1633(80)90058-1
12. Alov N. V. (2011): Development of methods of surface analysis in Russia.*Journal of Analytic Chemistry, 66*, 1073-1078. Doi: 10.1134/S1061934811110025
13. Alov N. V. (2011): Development of methods of surface analysis in Russia. *Journal of Analytic Chemistry, 66*, 1073-1078. Doi: 10.1134/S1061934811110025
14. Moghaddam S. A., Mattsson M., Ameen A., Akander J., Da Silva M.G., Simões N. (2021): Low-Emissivity Window Films as an Energy Retrofit Option for a Historical Stone Building in Cold Climate. *Energies 14*(22), 7584. Doi: 10.3390/en14227584
15. Nikitenkov N. (2017): Modern Technologies for Creating the Thin-film Systems and Coatings, *IntechOpen*, 10-45. Doi: 10.5772/63326
16. Jelle B. P., Kalnæs P. E., Gao T., (2015): Low-Emissivity Materials for Building Applications: A State-of-the-Art Review and Future Research Perspectives. *Energy and Buildings, 96*, 329–356. Doi: 10.1016/j.enbuild.2015.03.024
17. Kulczyk-Malecka J., Kelly P.J., West G. (2014): Investigation of silver diffusion in TiO$_2$/Ag/TiO$_2$ coatings. *Acta Materialia, 66*, 396–404. Doi: 10.1016/j.actamat.2013.11.030
18. Finley J. J., (1999): Heat treatment and bending of low-E glass. *Thin Solid Films, 351* (1-2), 264-273. Doi: 10.1016/S0040-6090(99)00087-5
19. Pilkington L. A. B. (1969): The float glass process. *The Royal Society, 314* (1516), 1-25. Doi: 10.1098/rspa.1969.0212
20. Schultz S. R. (2006): A glass float line simulation: modeling methodology and applications. *Conference: Procee-*

dings of the Winter Simulation Conference WSC 2006, Monterey, California, USA, December 3-6, 2006. Doi: 10.1145/1218112.1218241

21. Solntsev S. S., Rozenenkova V. A. (2006): Glass protective process coatings for heat treatment of steels and alloys. *Glass and ceramics, 63*(11), 386-390. Doi: 10.1007/s10717-006-0130-9
22. Xu J., Li Y. (2019): Manufacturing of Automotive Laminated Windshields. *Impact Behavior and Pedestrian Protection of Automotive Laminated Windshield*, 21-37. Doi: 10.1007/978-981-13-2441-3_2
23. Vakkuri E. Y., Kaonpää A., Salonen T., Nikkanen J., Method and furnace for bending glass sheets https://patents.google.com/patent/EP0592862A1, 1992.